Scientific-Coordination Workshop on Non-Ideal Plasma Physics ▪ 2024

Konyukhov A.V, Likhachev A.P. and Rostilov A.T.
Joint Institute for High Temperatures, Russian Academy of Sciences
Izhorskaya 13 Building 2, 125412 Moscow, Russia

Influence of thermodynamic non-ideality on cumulation in converging shock waves with symmetry violation

Abstract

Hydrodynamic simulations of initially perturbed converging cylindrical shock waves have been performed on moving (contracting) grids with equation of state accounting for hard-sphere repulsion on the basis of Carnahan-Starling approximation. Development of the converging shock wave instability connected with breaking of symmetry of radial flow has been studied. The flow was assumed to be adiabatic. Dependence upon packing density of hard spheres in the pre-shock state, that controls non-ideality in the hard-sphere model, is investigated. The symmetric converging shock waves in the hard-sphere fluid are found to have Guderley type power low asymptotics. It was found that the packing fraction has an effect on transverse shock waves formation and evolution. At high pre-shock density the calculations of cylindrical converging shock wave revealed its stability under strong initial perturbations of symmetry with the smallest angular period $\pi/2$: being polygonal-shaped due to strong initial perturbation the shock wave becomes cylindrical near the focus. For perturbations of particular form which have the smallest positive period π it was obtained that the shock waves are unstable in the whole region of stable fluid phase $0<\eta<0.5$. The instability is shown to be weaker for high values of the packing fraction.

Introduction

The converging shock waves (CSW) being a powerful tool for generation of high pressures and temperatures are of great interest in the high energy density physics and some applications. The CSW stability needed to provide efficient matter compression was studied by many authors both theoretically and experimentally. It was found the CSW in ideal or weakly non-ideal gas are unstable with respect to small symmetry violation. The influence of thermodynamic properties of shock compressed matter on the CSW stability remains unclear. It is reasonable to expect that this influence becomes increasingly sufficient as the CSW approaches to the centre of convergence. Some factors of the medium imperfection may be considered using van der Waals (vdW) equation of state (see, for instance, (Evance, 1996), (Wu, 1996), (Somogyi, 2007)), but post-shock densities interesting for research go beyond the feasibility of this approximation. More accurate results can be obtained on the basis of Carnahan-Starling (CS) equation of state (Carnahan, 1969) being valid at much higher compression degree. As well known, thermodynamic non-ideality of the hard-sphere system is characterized by the compressibility factor $Z=pV/RT$, which depends on the packing fraction $\eta=\pi D^3 N/(6V)$, here D is diameter of a sphere, N is a number of spheres in the volume V. In the case of the CS approximation $Z(\eta)=(1+\eta+\eta^2-\eta^3)/(1-\eta)^3$ (remind that for vdW equation of state $Z(\eta)=1/(1-4\eta)$). In our study hydrodynamic simulations of the CSW behavior have been performed on the basis of compressible Euler equations on moving grid with the equation of state accounting for hard-sphere repulsion in Carnahan-Starling approximation. Internal degrees of freedom were assumed to be frozen ($c_v=const$). Taking into account that CS fails to reproduce actual hard-sphere physics at $\eta>0.5$, such values of packing fraction were not used in calculations. The research is aimed to estimate influence of finite compressibility of matter on the CSW stability on the basis of simple tractable model.

Numerical method

For the purpose of accurate prediction of the converging shock wave the thin layer concluded between the shock wave surface and the limiting characteristic curve that comes to the point of reflection in R-t plane must be resolved numerically. For this purpose method of integration of the Euler equations on moving (contracting) grid has been applied, this approach has already been used in numerical modeling of the converging shock waves by other authors (see, for example [10]). Conservation of mass, momentum and energy for moving volume G can be written in the following form

$$\frac{d}{dt}\iiint_G \mathbf{U}d\omega + \iint_{\partial G}(\mathbf{F}_n - \mathbf{U}(\mathbf{v}_g\cdot\mathbf{n}))d\sigma = 0$$

where the vector $\mathbf{U}=(\rho,\rho\mathbf{v},\rho(e+{}^1\!/_2\mathbf{v}^2))^{\mathrm{T}}$ represents conservative variables, $\mathbf{F}_n(\mathbf{U},\mathbf{n})=(\rho v_n,\rho\mathbf{v}v_n,\rho v_n H)^{\mathrm{T}}$ - are the components of fluxes of the conservative variables in the direction of the external unit normal n of surface element $d\sigma$, is corresponding velocity component of volume G. Semi discrete approximation can be written as follows $v_{gn}=\mathbf{v}_g\cdot\mathbf{n}$.

$$\frac{d}{dt}(G\mathbf{U})_i = -\sum_j(\hat{\mathbf{F}}\cdot\mathbf{n})_j,\quad \frac{d}{dt}G_i = \sum_j(\mathbf{v}_g\cdot\mathbf{n})_j$$

where the index i denotes the values of grid functions, referred to the cell i, and summation is carried out over the cell faces, $\mathbf{n}_j$ is a normal, absolute value of which is equal to the area of the face j of the considered cell, the grid velocity vector $\mathbf{v}_g$ is evaluated at the face center. The modified fluxes at the cell faces of a smooth structured grid was approximated on the basis of the numerical flux developed by Harten and Yee and approximate Riemann problem solver of Glaister. All presented calculations were carried out with the use of the rectangular grids. Grid motion was defined by the following relation

$$\mathbf{x} = \mathbf{x}_0\exp\left(-\int_0^t c(\tau)d\tau\right),$$

where $c(t)$ controls the grid velocity $\mathbf{v}_g=-\mathbf{x}c(t)$. The front of the symmetrical convergent shock wave is steady on the moving grid if

$$c(t) = \frac{V_0}{R(t)}\left(\frac{p_1(t)-p_0}{V_0-V_1(t)}\right)^{1/2},$$

V_0, p_0 are the specific volume and pressure in pre-shock state, V_1, p_1 are the front parameters, R – current radius. Since in the case under consideration the shape of the shock wave and post-shock front parameters are perturbed, the averaging over N control points is used. The points are located on the shock front in such a way that angle between the points is φ/N, where φ - is the angular period of the perturbation of the shock wave.

$$c^{n+1} = (1-\omega)c^n + \omega c^*,\quad c^* = \sum_{k=1}^{N}\sigma_k\frac{V_0}{|\mathbf{x}_k|}\left(\frac{p_k-p_0}{V_0-V_k}\right)^{1/2},\quad k=1,2,\ldots N.$$

Here, σ_k are the weights. The parameters V_k, p_k, $\mathbf{x}_k$ are evaluated at the control points on time level n. The converging shock wave is generated by the break up of the initial discontinuity $\partial\Omega$, satisfying Rankine-Hugoniot jump conditions. The π – periodic perturbations was introduced by a small shift of the half-cylinders (half-spheres) along the cutting line (plane) on distance δr.

The hard-sphere EOS

The simple model taking into account repulsion forces

$$Z = \frac{pV}{nRT} = \frac{1+\eta+\eta^2-\eta^3}{(1-\eta)^3}$$

$$\eta = \frac{N_A\pi n\sigma^3}{6V}$$ - packing fraction

$$e = e(T)$$ - internal energy

In the present work $e=c_VT$, $c_V/R=5/3$

VALIDATION

Grid convergence
- Preservation of symmetry of CSW;
- Independence on orientation of the initial data on the computational grid

Comparison with Guderley's solution
Ideal gas, grid resolution: 400 cells per radius of the CSW. Guderley's similarity exponent n calculated from linear fit to the solution in $\log(r)$-$\log(p)$ plane:

Cylindrical wave

γ	Calculation	Theory [1]
5/3	0.816055	0.815625
7/5	0.835519	0.835217

Spherical wave

γ	Calculation	Theory [1]
5/3	0.688500	0.688377
7/5	0.717233	0.717173

For the given type of the perturbation solution of the problem depends on four dimensionless parameters: deviation of the shape from cylinder $\delta r/r_0$, dimensionless driving pressure p_1/p_0, and dimensionless pre-shock density η_0 that is exactly pre-shock packing fraction if $6m\pi/D^3$ is used as unit of density. Influence of η_0 and the type of perturbation was considered. In presented calculations the ratio p_1/p_0 was taken to be 160. Influence of the solution on $\delta r/r_0$ was not studied. This parameter was assumed to equal to 0.025. 2D calculations were performed on rectangular grid with resolution 400 cells per initial radius. Mesh 300x300x150 was used in 3D calculations with 100 computational cells per radius. Validation included tests on invariance of the solution with respect to orientation of the initial data on the rectangular grid, preserving of symmetry for unperturbed shock wave, and comparison with Guderley solution for the case of ideal gas. Figure 1 demonstrates independence of the solution on orientation of the cutting plane. The solutions correspond to turning of the initial data to the angle $\pi/4$ on rectangular grid. The lines of constant pressure are shown at scale 10^{-2}. Numerical solutions for different γ indicate nearly linear dependence in log scale at $r/r_0<10^{-1}$. Linear fit in the range $10^{-3}<r/r_0<10^{-2}$ gives the Guderley's exponent value within error 2% for the ideal gas.

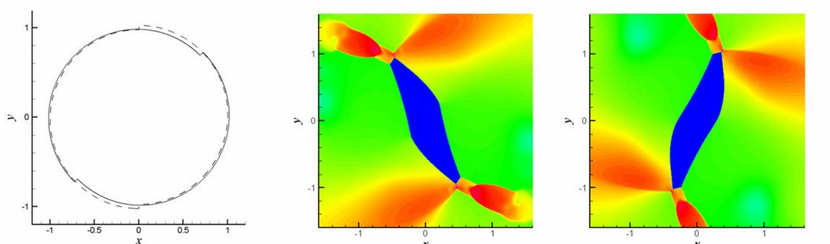

Figure 1 Invariance of the solution under rotation of the initial data to the angle $\pi/4$ on the rectangular grid. Cylindrical form of the discontinuity is perturbed by small shift (10 grid intervals) of half-cylinders along the cutting plane. Lines of constant pressure (the same in the both pictures) are presented at the moment when the size of the shock is approximately 10^{-2} (the units of length in the plots are 10^{-2} r_0).

Results

Consider the influence of the packing fraction on stability of the shape of the cylindrical converging shock wave in the case of the perturbations with angular period $\pi/2$. It is well known that in the case of ideal gas the perturbations with angular period $\pi/2$ increase in time. The instability leads to formation the shape of the shock front which is close to polygonal one. In particular, the initial phase of the instability development of this mode was observed in the experiment by Takayama et all [4]. Let us examine the front pressure history in the process of diminishing of its radius. The amplitude of fluctuations of front pressure can be estimated from difference of the front pressure at the two points (located on the shock wave front) such, that the angle between these points equals a half of the perturbation period. If the polygonal shape of the shock is formed, the front pressure is piecewise constant function of the distance from the focus. Discontinuity indicates existence of triple-points on the shock wave front.

If the pre-shock packing fraction is taken from the upper part of the interval of applicability of the CS equation of state, the cylindrical converging shock wave become stable against perturbations with period $\pi/2$. Moreover, stability is observed even in the case of strong initial asymmetry. Figure 2 shows the result for the case of strong initial perturbation, when the initial discontinuity is square in shape. It follows from the figure that the points of three-wave-configuration disappears from the surface of shock wave, and the growth rate of the average front pressure is higher than the growth rate of the front pressure perturbations. Initially polygonal shaped due to strong initial perturbation shock wave becomes cylindrical near the focus.

Calculations of the development of the shock wave perturbations characterized by the smallest positive period p have revealed that the cylindrical converging shock waves are unstable everywhere in the region of applicability of CS equation of state. Front pressure history at a pair of points is shown in figure 2 for each calculation. Represented data correspond to the following three values of the pre-shock packing fraction: η_0 = 0; 1/10; 1/3. The post-shock packing fraction approaches the strong shock limit. The values 0.217 and 0.444 where detected for η_0 = 1/10 and η_0 = 1/3, on the final stage of the calculations when the front pressure growth was completed. The front pressure histories for the unperturbed cylindrical shock waves which preserve its symmetry during implosion are shown by the dash-dot line.

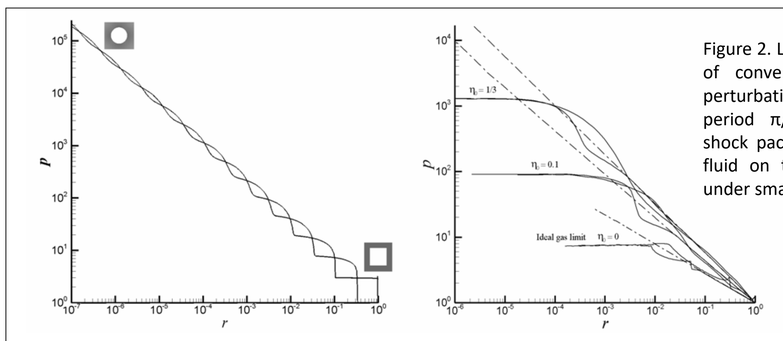

Figure 2. Left: case of stability of the cylindrical shape of converging shock wave under strong initial perturbations of symmetry with the smallest angular period $\pi/2$ (η_0 = 1/3); Right: Influence of the pre-shock packing fraction of spheres in a hard sphere fluid on the instability of converging shock wave under small initial perturbation with period π .

One can conclude from the figure that the front pressure follows the solution for the symmetric case in average until some critical value of pressure and radius is reached. This critical point depends on the packing fraction in the pre-shock state and coincides in time with formation of the quadruple points on the shock wave surface. Quadruple points are the stationary points on the shock wave surface where four shocks meet each other; two of them represent segments of the converging shock wave while the other two correspond to the outgoing shocks. In the particular case of symmetry this kind of shock interaction can be considered as a pair of regular shock reflections. Condition when this configuration appears from two triple points depends on criterion of transition from Mach reflection to regular one. It is known that the last condition depends on the thermodynamic properties of a medium. This type of shock interaction provides a mechanism of decreasing the area of the shock wave surface without increasing of the front pressure. Detailed pictures of the shock wave shape which it has at different scales are shown in figure 3 and figure 4 where the phenomenon is illustrated. The upper sequence of pictures in figure 3 correspond to an ideal gas, the lower one represents the case η_0 = 1/10. The last panel in each raw shows the shock front with quadruple points.

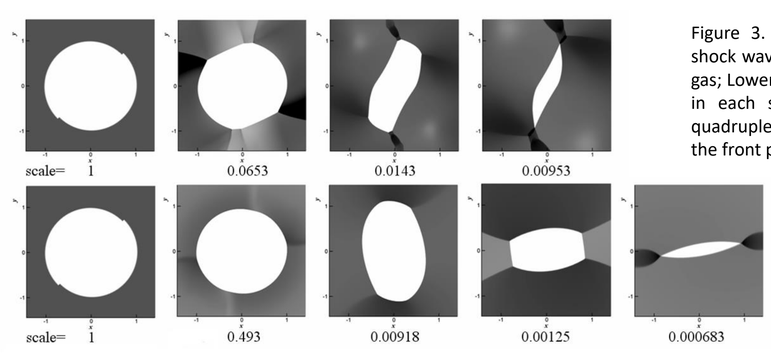

Figure 3. The shape of the perturbed converging shock wave at different scales is shown. Upper: ideal gas; Lower: hard sphere fluid η_0= 1/10. The last figure in each sequence corresponds to appearance of quadruple-shock-points on the shock wave surface; the front pressure does not grow after this moment.

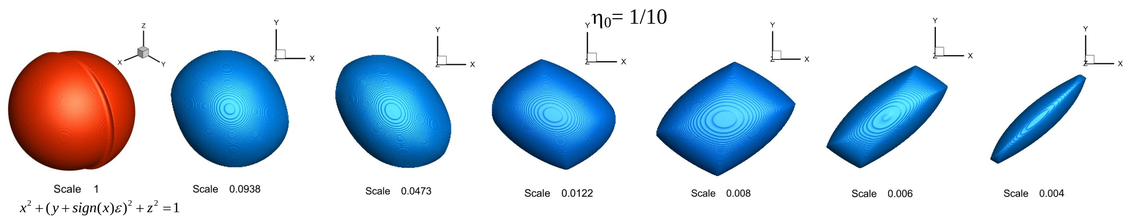

Figure 4. 3D calculation: the shape of the perturbed converging spherical shock wave at different scales is shown up to termination of the energy cumulation. Hard sphere fluid, η_0= 1/10, initial perturbation of the shock wave is defined by the shift of the focus at distance ε.

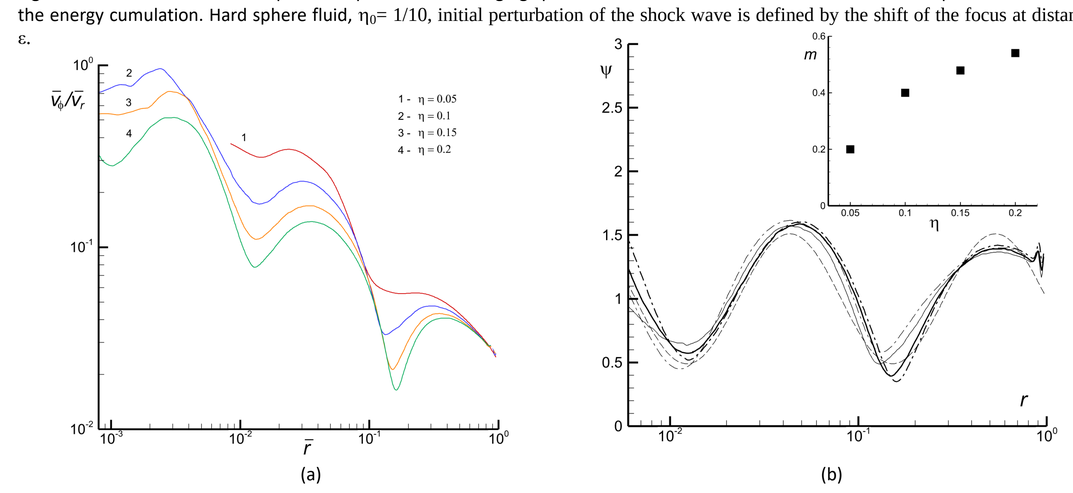

Figure 5. 3D calculation: (a) The influence of the initial density (in units of packing density of hard spheres) on the growth of the symmetry violation (in terms of the ratio of the average azimuthal velocity behind the shock wave to radial one) with decreasing distance to the focus; (б) dependence $\psi(r)=\varepsilon^{-1}(\bar{v}_\varphi/\bar{v}_r)r^{1-m}$ and parameter m for different values of the initial density and initial amplitude of the disturbance ε. The dashed curve corresponds to $\psi(r)=1+0.5\sin\left(\ln(r^{-5/2})\right)$.

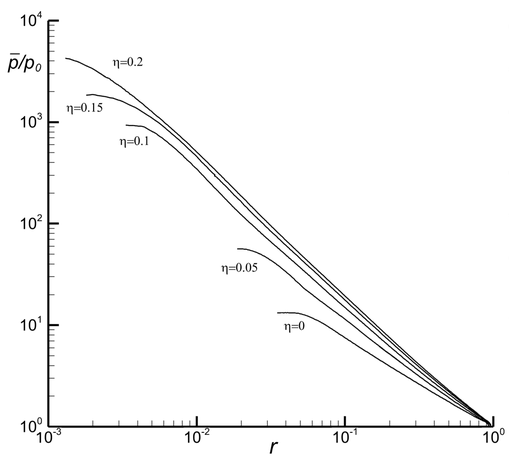

Figure 6. Pressure at shock-wave front vs radius

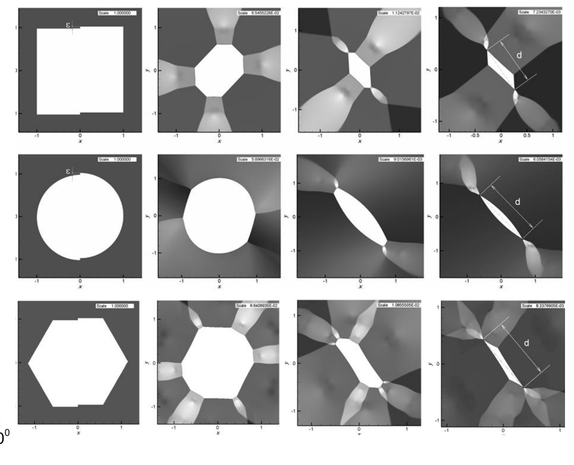

Figure 7. The influence of the higher perturbation modes

The relatively weak influence of higher perturbation modes on the development of the π –periodic perturbation in the cylindrical case is illustrated by calculations presented in figure 7. Taking into account data presented in figures 5 and 6 one can estimate the maximum of the pressure reached during the shock-wave compression by the following relation

$$p = p_0\left(\varepsilon_0/K\right)^{-\frac{n}{1-m}},\qquad \varepsilon_0 = (\bar{v}_\varphi/\bar{v}_r)_{r=r_0}$$

where n can be estimated from similarity solution for symmetrical converging shock wave, m is the increasing function of the packing fraction (figure 5b) and K is the ratio $\bar{v}_\varphi/\bar{v}_r$ at transition from Mach to regular reflection. For the sake of crude estimate one can take K=1.

In the hard-sphere fluid cylindrical shock wave, in contrast to the perfect gas, appears to be stable under the perturbations of symmetry, that have period $\pi/2$. The more dangerous mode, that is characterized by period π, is found to be unstable in entire range of liquid phase of the hard-sphere model.

References

1. Whitham, G. B., 1974 Linear and Non-linear Waves. NY: Wiley.
2. Schwendeman, D. W., Whitham, G. B. On converging shock waves // Proc. R. Soc. Lond. A. 1987. V. 413, P. 297-311.
3. Wu J.T., Neemeh R.A., Ostrowski P.P. Experiments on the stability of converging cylindrical shock waves // AIAA J. 1981. V. 19. P. 257-258.
4. Takayama K. et al Experiments on the stability of converging cylindrical shock waves// Theor. Appl. Mech. 1984. V. 32. P. 305-329.
5. Watanabe M. and Takayama K. Stability of converging cylindrical shock waves // Shock Waves. 1991. V. 1: P. 149.
6. Wu C.C., Roberts P.H. Structure and stability of a spherical shock wave in a van der Waals gas // Quarterly Journal of Mechanics and Applied Mathematics. 1996. V. 49 (4) P. 501-543
7. Somogyi Z., Roberts P.H. Stability of an imploding spherical shock wave in a van der Waals gas II // Quarterly Journal of Mechanics and Mechanics Appl Math. 2007. V. 60 (3)289-309.
8. Zhakhovskii, V., Nishihara, K. & Abe, M. 2002 Molecular Dynamics Simulation on Stability of Converging Shocks. Proc. of the 2nd Int. Conference on Inertial Fusion Science and Applications. Kyoto, Japan, Sept.9-14, 2001 Phys., Paris: Elsevier, pp. 106-109.
9. Carnahan N. F. & Starling K. E., 1969, J. Chem. Phys., vol. 51 p.635.